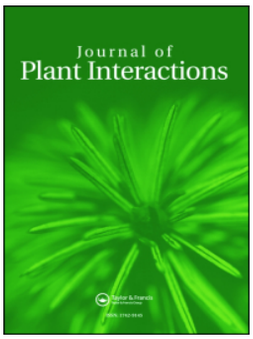

Journal of Plant Interactions

ISSN: (Print) (Online) Journal homepage: https://www.tandfonline.com/loi/tjpi20

Bicarbonate uptake experiment show potential karst carbon sinks transformation into carbon sequestration by terrestrial higher plants

Lei Fang & Yanyou Wu

To cite this article: Lei Fang & Yanyou Wu (2022) Bicarbonate uptake experiment show potential karst carbon sinks transformation into carbon sequestration by terrestrial higher plants, Journal of Plant Interactions, 17:1, 419-426, DOI: 10.1080/17429145.2022.2045369

To link to this article: https://doi.org/10.1080/17429145.2022.2045369

© 2022 The Author(s). Published by Informa UK Limited, trading as Taylor & Francis Group

Published online: 02 Mar 2022.

Submit your article to this journal

Article views: 1109

View related articles

View Crossmark data

Citing articles: 2 View citing articles

Full Terms & Conditions of access and use can be found at
https://www.tandfonline.com/action/journalInformation?journalCode=tjpi20

JOURNAL OF PLANT INTERACTIONS
2022, VOL. 17, NO. 1, 419–426
https://doi.org/10.1080/17429145.2022.2045369

Taylor & Francis
Taylor & Francis Group

PLANT-ENVIRONMENT INTERACTIONS

OPEN ACCESS Check for updates

Bicarbonate uptake experiment show potential karst carbon sinks transformation into carbon sequestration by terrestrial higher plants

Lei Fang[a,b] and Yanyou Wu[a]

[a]State Key Laboratory of Environmental Geochemistry, Institute of Geochemistry, Chinese Academy of Sciences, Guiyang, People's Republic of China; [b]University of Chinese Academy of Sciences, Beijing, People's Republic of China

ABSTRACT

Karstification forms tremendous karst carbon sinks in the Earth. Whether terrestrial higher plants can absorb and utilize bicarbonate, there is a key testimony that karst carbon sinks can be transformed into carbon sequestrations by terrestrial higher plants. The uptake and use of root-derived bicarbonate, photosynthesis, phosphoenolpyruvate carboxylase and ribulose-1,5-bisphosphate carboxylase contents of *Broussonetia papyrifera* (*Bp*) and *Morus alba L.* (*Ma*) were measured. This study provides the most direct and primary evidence for the transformation using the bidirectional isotope tracer technique. The transformation may result from the synergism in the absorption and utilization of photosynthetic and nonphotosynthetic pathway, and simultaneously strengthen karst carbon sink and carbon sequestrations of plants, while it had no effect on photosynthetic CO_2 assimilation in leaves. Differences in the transformation result in the discrepancies of *Bp* and *Ma* in the adaptation to karst environments. Karst-adaptable plants can more regulate the entire carbon cycle.

ARTICLE HISTORY
Received 10 November 2021
Accepted 17 February 2022

KEYWORDS
Carbon neutrality; inorganic carbon; photosynthesis; isotope tracer technique; carbon dissolution

1. Introduction

For a long time, global major carbon pools, carbon sources, carbon sinks and carbon budgets have attracted much attention (Raymond *et al.* 2013; Friedlingstein *et al.* 2020; Luo *et al.* 2020; Ran *et al.* 2021). The overall average time of global carbon turnover is 23 (+7) years (95% confidence interval), and carbon turnover in many semiarid regions is faster (Carvalhais *et al.* 2014). The carbon sinks of exposed areas of carbonate rocks in China account for 177×10^{11} g CO_2/a (Jiang and Yuan 1999). With climate warming, high temperatures increase rock weathering, and the CO_2 consumption rate of carbonate rock weathering is 6.248×10^{11} g CO_2/a (Liu *et al.* 2021). Plants can effectively promote long-term carbon storage by directly accumulating and fixing organic carbon in their ecosystems. More than one-third of the CO_2 in the atmosphere is exchanged annually with the terrestrial biosphere through stomata into leaves and the leaf water solution, and approximately half of this carbon is fixed during photosynthesis (Farquhar *et al.* 1993; Ciais *et al.* 1997). The CO_2 exchange of leaves is approximately 15 μmol m^{-2} s^{-1} at 25° C, and more than half of the carbon fixed by plants in a year is consumed by plant respiration (Wang *et al.* 2001). The carbon exchange capacity of plants is less affected by environmental changes and temperature at the annual scale, and physiological processes controlling water loss during carbon uptake reach a sustainable balance throughout the year (Law *et al.* 2002), so the carbon exchange of photosynthesis is relatively stable. With the increase of plant coverage, both the net primary productivity (NPP) and net ecosystem productivity (NEP) of land has increased (Cao *et al.* 2003; Zhu *et al.* 2016; Lu *et al.* 2018). In karst regions, above-ground biomass carbon increased by 9% under drought conditions (Tong *et al.* 2018).

The carbon cycle is a key process of terrestrial ecosystem changes. Typically, photosynthesis plays an important role in adjusting to climate change by fixing CO_2 in the atmosphere through stomata and converting it into organic matter. However, the rock exposure rate in karst regions is high, and rainwater enters groundwater from rock crevices, resulting in a two-dimensional structure of water and soil separation, which makes water and soil loss occur easily (Wang *et al.* 2004; Van Beynen and Townsend 2005; Yan *et al.* 2012). Due to the unique features of karst regions, plants often root in cracks, resulting in a complex plant-soil-rock structure. The plants are thus exposed to $CaCO_3 + H_2O + CO_2 \rightarrow Ca^{2+} + 2HCO_3^-$ for a long time. HCO_3^- is the main anion present in the soil solution of calcareous soils (Yan *et al.* 2012). The climate in karst regions of Guizhou Province, China, is humid year-round. In humid and anoxic soil environments, the HCO_3^- concentration can reach 5 mM or even 10 mM (Boxma 1972; Bloom and Inskeep 1986).

The interaction between CO_2 sequestration of plants and karst carbon sinks has a great impact on the carbon pool of terrestrial ecosystems. In karst regions, $CO_2 + H_2O \rightleftharpoons HCO_3^- + H^+$ maintains a dynamic balance, and it is difficult to determine whether karst carbon sinks are transformed into CO_2 sequestrations. Previous work has demonstrated the absorption and utilization of bicarbonate at the leaf level (Wu and Xing 2012; Rao and Wu 2017), but more direct evidence from roots is lacking. The two Moraceae species studied here, *Broussonetia papyrifera* (*Bp*) and *Morus alba L.* (*Ma*), have different adaptability to low nutrient and excess HCO_3^- environments, and *Bp* is a karst-adaptable plant because of its good adaptability to karst soil (Zhao and Wu 2017; Yao and Wu 2021). Whether plants can

CONTACT Yanyou Wu wuyanyou@mail.gyig.ac.cn State Key Laboratory of Environmental Geochemistry, Institute of Geochemistry, Chinese Academy of Sciences, No. 99 Lincheng West Road, Guanshanhu District, Guiyang, Guizhou Province 550081, People's Republic of China

© 2022 The Author(s). Published by Informa UK Limited, trading as Taylor & Francis Group
This is an Open Access article distributed under the terms of the Creative Commons Attribution License (http://creativecommons.org/licenses/by/4.0/), which permits unrestricted use, distribution, and reproduction in any medium, provided the original work is properly cited.

absorb and use bicarbonate is one of the key points in proving the transformation of karst carbon sinks into carbon sequestrations of terrestrial higher plants. Moreover, it is of great significance to understand the utilization of inorganic carbon by plants as an additional carbon source for supplementary photosynthesis. This study provides a direct, rapid and nondestructive method for quantifying the bicarbonate absorption capacity of plants and observes the response of plants to photosynthetic CO_2 assimilation during bicarbonate absorption under different photoperiods.

2. Materials and methods

2.1. Plant materials

The experiment was conducted in an artificial climate chamber of the Institute of Geochemistry, Chinese Academy of Sciences, Guiyang, China. Seeds of *Bp* and *Ma* were germinated in a greenhouse on a mixture of perlite and vermiculite. The germinated seeds of *Bp* and *Ma* were subsequently cultivated in 1/2-strength modified Hoagland solution for 10 months and 5 months, respectively, until the plant height was 52–57 cm. Seedlings with a similar size were used for the experiment. All plants for the experiment were grown under controlled environmental conditions in a greenhouse under a 12-h photoperiod (500 ± 50 μmol m^{-2} s^{-1}, photosynthetically active radiation) and a temperature of 25°C/20°C (light/dark). Relative humidity was maintained at 50%–55%.

2.2. Absorption experiment of bidirectional isotope tracer culture

This experiment was divided into 2 labeling groups, 3 treatments, and 3 replicates for each treatment. The absorption solution was 2 L of the modified Hoagland nutrient solution supplemented with 10 mM $NaHCO_3$ with different $\delta^{13}C$ values, 4.00‰ (labeled 1) and −27.07‰ (labeled 2). The pH of the absorption solution was adjusted to 8.30 ± 0.05, which can maintain most HCO_3^- in this range (Millero 2014). Sixty-five milliliters of absorption solution was used to measure the $\delta^{13}C$ of dissolved inorganic carbon (DIC). The 3 treatments were a 12-h photoperiod (control), 24 h of continuous light after 12 h of darkness (24L) and 24 h of continuous dark after 12 h of illumination (24D). The same plants were used for labeled groups 1 and 2. No plant was placed in the bidirectional isotope trace blank culture system (blank). In the control, *Bp* was selected from the root/shoot ratio (R/S) value of approximately 0.5. In 24L and 24D, *Bp* was selected from the R/S value of approximately 1.0. The DIC measurement was performed on a gas isotope mass spectrometer (MAT252, Finnigan, Germany). Vacuumed the sealed bottle containing 2–3 ml phosphoric acid and injected absorption solution for full reaction. CO_2 produced by the reaction was purified and then measured $\delta^{13}C$ values. The volume of solution at the end of the experiment was measured.

2.3. Leaf gas exchange

The CO_2 assimilation rate (Ac), stomatal conductance (gs) and transpiration rate (Tr) were measured after treatment (control and 24L) by a portable photosynthesis measurement system (Li-6400; Li-Cor, Lincoln, NE). The PPFD was set at 500 μmol m^{-2} s^{-1}, and the CO_2 concentration was 380 μmol m^{-2} s^{-1}. The water-use efficiency (WUE) was calculated as follows: WUE = Pn/Tr. The 24D treatment group was exposed to 500 ± 50 μmol m^{-2} s^{-1} light for one hour prior to measurement, and the remaining steps were the same.

2.4. Chlorophyll fluorescence

Chlorophyll fluorescence was measured after the determination of leaf gas exchange by a portable photosynthesis system (Li-6400; Li-Cor, Lincoln, NE). First, the minimum initial chlorophyll fluorescence (F_o) and maximum chlorophyll fluorescence (F_m) of the plants were measured after dark adaptation for more than 30 min. Subsequently, the maximum fluorescence (F'_m) of plants and the steady-state yield of fluorescence (F_s) in the light were measured after the plants were photoactivated for 1 h, at which point the photosynthetic photon flux density (PPFD) was set at 200 μmol m^{-2} s^{-1}. The photosystem II potential photochemical quantum efficiency (F_v/F_m), the efficiency of photosystem II photochemistry (φPSII) and the electron transfer rate (ETR) can be calculated (Weis and Berry 1987; Maxwell and Johnson 2000).

2.5. PEPC and Rubisco

The phosphoenolpyruvate carboxylase (PEPC) and bibulose-1,5-bisphosphate carboxylase (Rubisco) contents under the 3 treatments (control, 24L and 24D) were measured by a double antibody one-step cascade enzyme-linked immunosorbent assay (ELISA). Samples, standards and horseradish peroxidase (HRP)-labeled detection antibodies were successively added to micropores precoated with PEPC and Rubisco antibodies, which were incubated and thoroughly washed. Tetramethylbenzidine (TMB) is a chromogenic substrate and changes color from blue to yellow. The intensity of color was positively correlated with the concentrations of PEPC and Rubisco in the sample. The optical density (OD) was measured at 450 nm using a microplate spectrophotometer. The concentrations of PEPC and Rubisco in the sample were then determined by comparing the OD of the samples to the standard curve. The measured samples were fresh roots, stems and leaves of plants stored in a refrigerator at −80°C until analysis.

2.6. Calculation of bicarbonate absorption

The strong fractionation characteristics of stable carbon isotopes facilitate the identification of different inorganic carbon sources. The bivariate isotope-mixture model can be expressed as

$$\delta_i = \delta_{Ca} - f_{Bi}\delta_{Ca} + f_{Bi}\delta_{Ci} \quad (1)$$

where δ_i is the $\delta^{13}C$ value of inorganic carbon in the culture medium at a certain period of time in cultured plants, δ_{Ca} is the $\delta^{13}C$ value of inorganic carbon dissolved in the culture solution from CO_2 in the air, δ_{Ci} is the $\delta^{13}C$ value of bicarbonate in the initial culture solution, and f_{Bi} is the proportion of added exogenous bicarbonate accounting for the total inorganic carbon sources in the culture solution at a certain period of time.

For labeled 1, Eq. 1 can be rewritten as follows:

$$\delta_1 = \delta_{Ca} - f_{B1}\delta_{Ca} + f_{B1}\delta_{C1} \quad (2)$$

For labeled 2, Eq. 1 can be rewritten as follows:

$$\delta_2 = \delta_{Ca} - f_{B2}\delta_{Ca} + f_{B2}\delta_{C2} \quad (3)$$

Comparing Eqs. 2 and 3, $f_B = f_{B1} = f_{B2}$; thus, Eqs. 2 and 3 can be used for the following calculations:

$$f_B = \frac{\delta_1 - \delta_2}{\delta_{C1} - \delta_{C2}} \quad (4)$$

where f_B is the proportion of added exogenous bicarbonate accounting for the total inorganic carbon sources in the plant culture system at a certain period of time, δ_1 is the $\delta^{13}C$ value of inorganic carbon in the culture medium at a certain period of time in labeled 1, δ_2 is the $\delta^{13}C$ value of inorganic carbon in the culture medium at a certain period of time in labeled 2, δ_{C1} is the $\delta^{13}C$ value of bicarbonate in the initial culture solution in labeled 1, and δ_{C2} is the $\delta^{13}C$ value of bicarbonate in the initial culture solution in labeled 2.

In the blank culture system, the added exogenous bicarbonate ions can be exchanged with CO_2 in the air. After a period of consumption, the proportion of added exogenous bicarbonates accounting for the total inorganic carbon source in the blank culture system can be represented as follows:

$$f_0 = \frac{\delta_{01} - \delta_{02}}{\delta_{C1} - \delta_{C2}} \quad (5)$$

In the bidirectional isotope trace plant and blank culture system under the different time periods Eqs. 4 and 5 can be rewritten as

$$f_{Bi} = \frac{\delta_{1i} - \delta_{2i}}{\delta_{C1} - \delta_{C2}} \quad (6)$$

$$f_{0i} = \frac{\delta_{01i} - \delta_{02i}}{\delta_{C1} - \delta_{C2}} \quad (7)$$

where i is the sampling time.

In the bidirectional isotope trace blank culture system under the different time periods, the cumulative bicarbonate consumption amount (m_i) can be calculated as follows:

$$m_i = (cv_0 f_{00} - cv_{0i} f_{0i}) - d_i^0 \quad (8)$$

where c is the initial concentration of bicarbonate set at 10 mM, v_{0i} is the volume of the culture solution at different times, f_{00} is the proportion of the labeled bicarbonate in the initial culture solution, and d_i^0 is cumulative sampling consumption.

In the bidirectional isotope trace plant culture system under the different time periods, the cumulative bicarbonate consumption amount (p_i) can be rewritten as

$$p_i = (cv_0 f_{B0} - cv_{1i} f_{Bi}) - d_i^1 \quad (9)$$

where c is the initial concentration of bicarbonate set at 10 mM, v_{1i} is the volume of the culture solution at different times, f_{B0} is the proportion of the labeled bicarbonate in the initial culture solution, and d_i^1 is cumulative sampling consumption.

In the bidirectional isotope trace blank culture system under the different time periods, d_i^0 can be calculated as follows:

$$d_i^0 = d_{i-1}^0 + cv_d f_{0i} \quad (10)$$

where v_d is the sampling volume, d_0^0 is 0, and d_{i-1}^0 is the last cumulative sampling consumption.

In the bidirectional isotope trace plant culture system under the different time periods, d_i^1 can be written as

$$d_i^1 = d_{i-1}^1 + cv_d f_{Bi} \quad (11)$$

where v_d is the sampling volume, d_0^1 is 0, and d_{i-1}^1 is the last cumulative sampling consumption.

In the bidirectional isotope trace blank culture system under the different time periods, the cumulative consumption amount of dissolved bicarbonate from the air (n_i) can be calculated as follows:

$$n_i = m_i \frac{(1 - f_{0i})}{f_{0i}} \quad (12)$$

In the bidirectional isotope trace blank culture system under the different time periods, the cumulative consumption amount of total bicarbonate (a_0) can be calculated as follows:

$$a_0 = m_i + n_i \quad (13)$$

In the bidirectional isotope trace plant culture system under the different time periods, the cumulative consumption amount of dissolved bicarbonate from the air (q_i) can be written as

$$q_i = p_i \frac{(1 - f_{Bi})}{f_{Bi}} \quad (14)$$

In the bidirectional isotope trace plant culture system under the different time periods, the cumulative consumption amount of total bicarbonate (b_0) can be written as

$$b_0 = p_i + q_i \quad (15)$$

A linear relationship model between a_0, b_0 and absorption time was constructed, and the slope of the model was the consumption rate of the total bicarbonate in the bidirectional isotope trace culture systems. The bicarbonate absorption rate (V_b) of the plant was calculated as

$$V_b = V_1 - V_0 \quad (16)$$

where V_1 is the consumption rate of the total bicarbonate in the bidirectional isotope trace plant culture systems, and V_0 is the consumption rate of the total bicarbonate in the bidirectional isotope trace blank culture systems.

After the treatment, the shoot fresh weight (Sfw) was measured. The bicarbonate absorption rate of shoots (V_{SFW}) was calculated as follows:

$$V_{SFW} = \frac{V_b}{Sfw} \quad (17)$$

2.7. Statistical analysis

All measurements were subjected to analysis of variance (ANOVA). The means of the different groups were compared *via* Duncan's multiple range tests. Tests were considered significant at the $p < 0.05$ level. Data are shown as the mean ± the standard error (SE). Statistical analyses were carried out with SPSS software (version 25, IBM.).

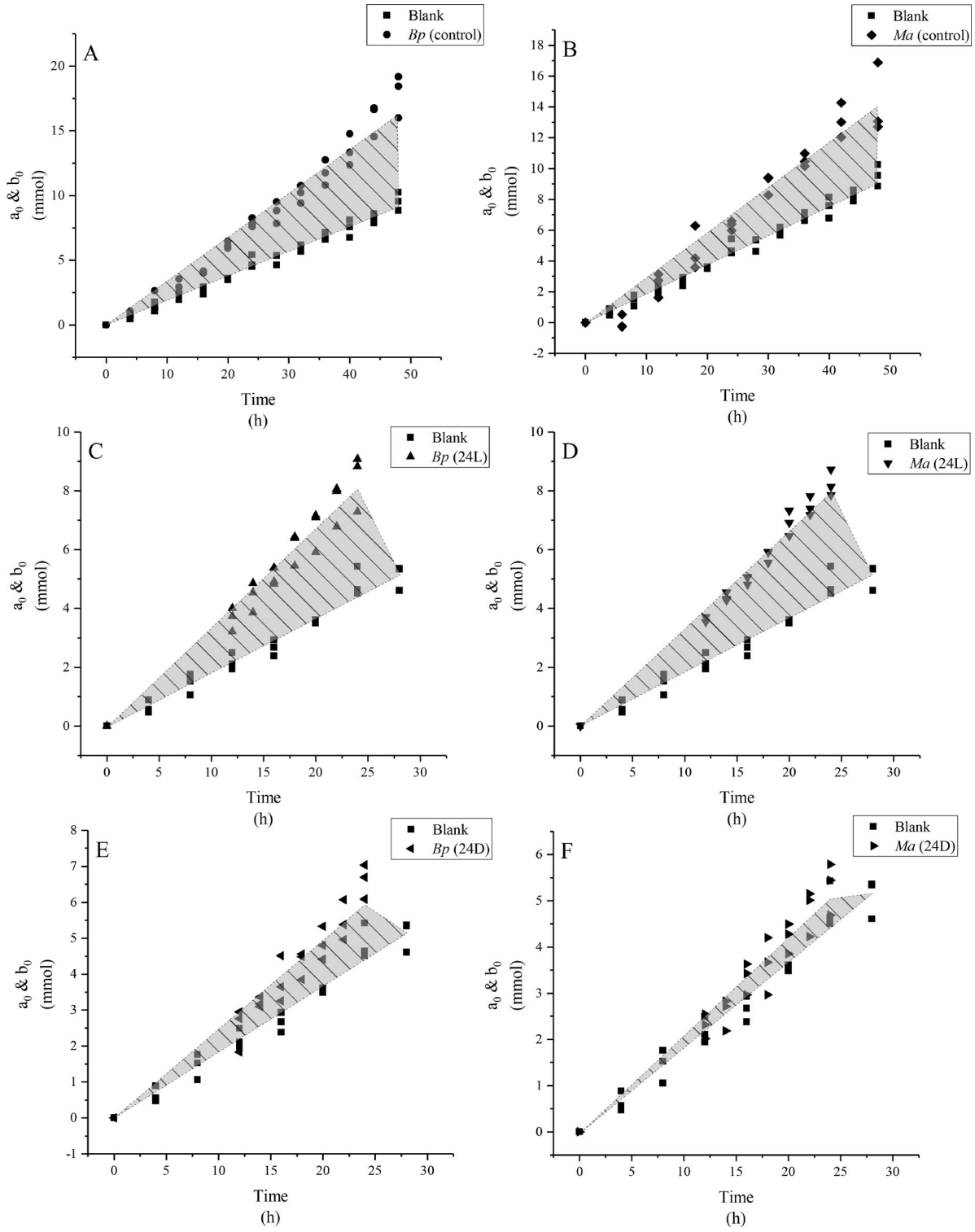

Figure 1. a_0 and b_0 of *Bp* and *Ma* in the fitting linear relationship between the cumulative amount of total bicarbonate consumed and absorbed time under the control (A and B), 24L (C and D) and 24D (E and F), respectively.

Note: The shadow part represents the plant absorption rate of bicarbonate (Vb). a0, the cumulative consumption amount of total bicarbonate in the bidirectional isotope trace blank culture system; b0, the cumulative consumption amount of total bicarbonate in the bidirectional isotope trace palnt culture system.

Linear fitting analyses and graphing were carried out with Origin software (version 9.4, OriginLab.).

3. Results

3.1. Absorption of bicarbonate by plants

The linear fitting results of the changes in a_0 and b_0 showed discrepancies in the different treatments of the two plant species (Figure 1). In the control, the V_b of *Bp* is higher than that of *Ma*. The V_b of *Bp* was higher under the control and 24L than 24D, and there was no significant difference between the control and 24L. The V_b of *Bp* under the control and 24L were 2.5 times that under 24D. The V_b of *Ma* was higher under the control and 24L than 24D, there is no significant difference between the control and 24L, and the V_b of *Ma* under the control and 24L were 5 and 7 times that under 24D, respectively. Through the results of the linear fitting analysis (Table 1), there is an excellent linear proportional relationship between V_{SFW} and absorbed time,

Table 1. The consumption rate of the total bicarbonate in blank and plant culture system under the control, 24L and 24D.

	Equation		R^2		V_0 & V_1		V_{SFW} (μ mol/h.g)	
Blank	Y = 0.1848X		0.99		0.19 ± 0.01		–	
	Y = 0.1848X		0.98					
	Y = 0.1986X		0.99					
	Bp	*Ma*	*Bp*	*Ma*	*Bp*	*Ma*	*Bp*	*Ma*
Control	Y = 0.3522X	Y = 0.3122X	0.96	0.95	0.34 ± 0.02	0.29 ± 0.02	6.64 ± 1.16b	7.47 ± 0.68b
	Y = 0.3118X	Y = 0.2768X	0.98	0.95				
	Y = 0.3522X	Y = 0.2885X	0.97	0.95				
24L	Y = 0.2984X	Y = 0.3339X	0.99	0.98	0.34 ± 0.03	0.33 ± 0.01	4.46 ± 0.82c	10.38 ± 0.52a
	Y = 0.3570X	Y = 0.3171X	0.99	0.99				
	Y = 0.3521X	Y = 0.3424X	0.98	0.98				
24D	Y = 0.2662X	Y = 0.1886X	0.98	0.95	0.25 ± 0.02	0.21 ± 0.02	1.77 ± 0.76d	1.75 ± 1.81d
	Y = 0.2228X	Y = 0.2137X	0.94	0.97				
	Y = 0.2537X	Y = 0.2267X	0.96	0.99				

Note: The data are expressed as mean ± standard error ($M \pm SE$). The same letter means no significant difference (Duncan's multiple range tests, $P < 0.05$). V_0, the bicarbonate consumption rate in the bidirectional isotope trace blank culture system; V_1, the bicarbonate consumption rate in the bidirectional isotope trace plant culture system; V_{SFW}, bicarbonate absorption rate of shoot.

Table 2. Leaf gas exchange and chlorophyll fluorescence under the control, 24L and 24D.

	Bp			*Ma*		
	Control	24L	24D	Control	24L	24D
Ac	8.22 ± 0.76a	1.21 ± 0.21d	2.75 ± 0.66c	5.44 ± 0.32b	6.24 ± 0.47b	8.04 ± 0.51a
gs	0.09 ± 0.03a	0.01 ± 0.00b	0.02 ± 0.01b	0.05 ± 0.01ab	0.08 ± 0.01a	0.08 ± 0.01a
Tr	1.86 ± 0.44a	0.24 ± 0.05d	0.42 ± 0.12cd	0.93 ± 0.11bc	1.37 ± 0.21ab	1.29 ± 0.10ab
WUE	4.88 ± 0.53b	5.71 ± 0.85ab	7.08 ± 0.77a	6.16 ± 0.68ab	4.85 ± 0.39b	6.31 ± 0.43ab
F_v/F_m	0.70 ± 0.02a	0.53 ± 0.08b	0.72 ± 0.01a	0.73 ± 0.01a	0.60 ± 0.01b	0.59 ± 0.03b
φPSII	0.62 ± 0.03a	0.51 ± 0.08a	0.56 ± 0.05a	0.56 ± 0.01a	0.55 ± 0.03a	0.61 ± 0.01a
ETR	52.19 ± 3.09a	43.11 ± 6.97a	47.44 ± 4.26a	47.80 ± 1.19a	46.30 ± 3.14a	51.63 ± 0.84a

Note: The data are expressed as mean ± standard error ($M \pm SE$). The same letter means no significant difference (Duncan's multiple range tests, $P < 0.05$). Ac, CO_2 assimilation rate; gs, stomatal conductance; Tr, transpiration rate; WUE, water-use efficiency; F_v/F_m, photosystem II potential photochemical quantum efficiency; φPSII, efficiency of photosystem II photochemistry; ETR, electron transfer rate. * Values of Ac, gs and Tr were reported in $\mu molm^{-2}\ s^{-1}$, mol $H_2Om^{-2}\ s^{-1}$ and mmol $H_2Om^{-2}\ s^{-1}$, respectively.

Table 3. The content of PEPC and Rubisco in roots (R), stems (S) and leaves (L) under the control, 24Land 24D.

		Bp			*Ma*		
		Control	24L	24D	Control	24L	24D
PEPC	L	0.9 ± 0.12a	0.94 ± 0.11a	0.82 ± 0.10a	0.85 ± 0.09a	0.91 ± 0.13a	0.87 ± 0.15a
	S	0.77 ± 0.08a	0.78 ± 0.10a	0.67 ± 0.18a	0.73 ± 0.19a	0.81 ± 0.04a	0.68 ± 0.16a
	R	0.49 ± 0.04b	0.48 ± 0.06b	0.56 ± 0.07ab	0.58 ± 0.09ab	0.50 ± 0.09b	0.64 ± 0.07a
Rubisco	L	0.70 ± 0.04ab	0.64 ± 0.06b	0.81 ± 0.04a	0.72 ± 0.16ab	0.77 ± 0.04ab	0.75 ± 0.09ab
	S	0.64 ± 0.05abc	0.67 ± 0.04ab	0.56 ± 0.09c	0.52 ± 0.05bc	0.69 ± 0.06a	0.59 ± 0.11abc
	R	0.36 ± 0.05a	0.32 ± 0.09a	0.34 ± 0.12a	0.37 ± 0.03a	0.37 ± 0.11a	0.24 ± 0.04a

Note: The data are expressed as mean ± standard error ($M \pm SE$). The same letter means no significant difference (Duncan's multiple range tests, $P < 0.05$). *Values of PEPC and Rubisco content were reported in U/g.

and the square values of the correlation coefficient (R^2) exceed 0.94. In the control, there is no significant difference between the V_{SFW} of *Bp* and *Ma*. The V_{SFW} of *Bp* was highest under the control and was 1.5 and 3.8 times that of 24L and 24D, respectively. The V_{SFW} of *Bp* under 24L was 2.5 times that of 24D. The V_{SFW} of *Ma* was highest in 24L and was 1.4 and 5.9 times that of the control and 24D, respectively. The V_{SFW} of *Ma* under the control was 4.3 times that of 24D.

3.2. Photosynthetic CO_2 assimilation

Leaf gas exchange and chlorophyll fluorescence represent photosynthetic CO_2 assimilation. As shown in Table 2, the Ac, gs, and Tr of *Bp* were highest, while the WUE was lowest under the control. The Ac of *Bp* under 24L was lower than that under 24D. gs, Tr and WUE of *Bp* were not significantly different between 24L and 24D. The Ac of *Ma* was highest under 24D and had no significant differences between the control and 24L. gs, Tr and WUE of *Ma* had no significant differences among the 3 treatments. φPSII and ETR of the two plant species had no significant differences among the 3 treatments. The F_v/F_m of *Bp* under the control and 24D treatments was significantly higher than that under 24L. The F_v/F_m of *Ma* was highest under the control.

3.3. PEPC and Rubisco

PEPC and Rubisco were found in roots, stems and leaves under the 3 treatments, but there was a discrepancy between the two plant species under different treatments. As shown in Table 3, the PEPC of the stems and leaves of the two plant species were not significantly different among the 3 treatments. The PEPC of *Bp* roots was not significantly different among the 3 treatments. The PEPC of *Ma* roots under 24L was 78% that under 24D. There was more PEPC in the shoots of plants than in the roots. Rubisco in the roots had no significant difference between *Bp* and *Ma* among the 3 treatments. Rubisco of *Bp* stems was lower under 24D than 24L. The Rubisco of *Ma* stems was higher under the 24L than control. The Rubisco of *Bp* leaves under 24L was 79% that under 24D. The Rubisco of *Ma* leaves had no significant difference among the 3 treatments. There was more Rubisco in the shoots of plants than in the roots.

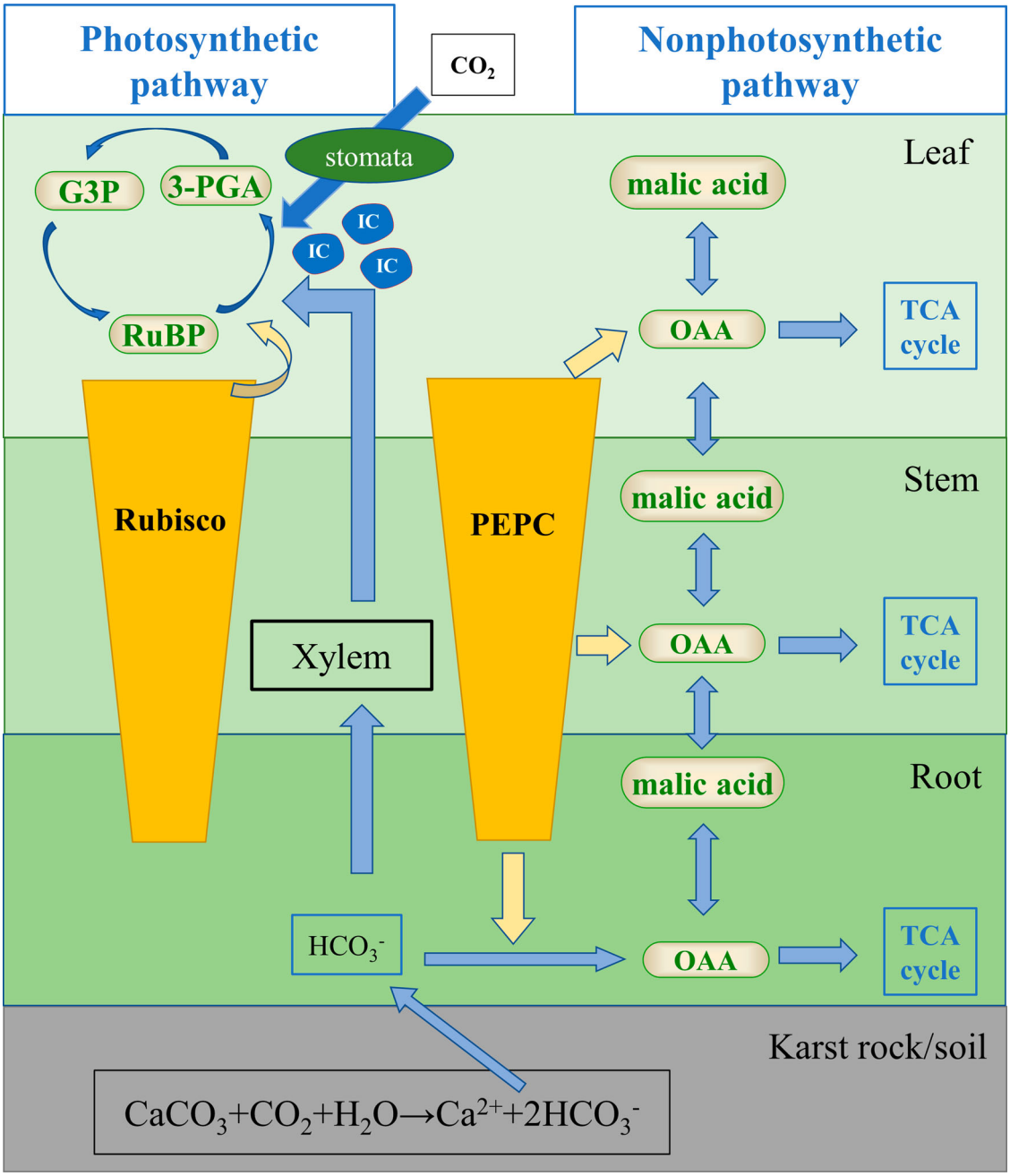

Figure 2. Hypothetical schematic model of PEPC and Rubisco response to bicarbonate in plants.

Note: Bicarbonate uptake by plants via photosynthetic and nonphotosynthetic pathways under light, and only nonphotosynthetic pathway under dark. IC, inorganic carbon; RUBP, ribulose-1,5-bisphosphate; 3-PGA, 3-phosphoglycerate; G3P, glyceraldehyde 3-phosphate; OAA, oxaloacetic acid; TCA cycle, tricarboxylic acid cycle.

4. Discussion

This study demonstrates that plants absorb and utilize considerable amounts of bicarbonate under both light and dark conditions, indicating that karst carbon sinks can be converted into carbon sequestrations by plants during all times of day. The absorption of bicarbonate with first-order reaction kinetics reveals that plants can absorb and utilize root-derived HCO_3^- in addition to use CO_2 from the air (Figure 1). Meanwhile, bicarbonate can be absorbed and utilized by the nonphotosynthetic pathway in the dark in addition to *via* photosynthesis. Inorganic carbon sequestration *via* these two pathways is a key mechanism for plant adaptation to karst environments. However, the bicarbonate uptake of *Bp* and *Ma* was different (Table 1), which may cause discrepancies in the adaptation to the karst environment in the two plant species.

This study also showed that inorganic carbon sequestration from karst carbon sinks was independent of CO_2 assimilation. *Bp* had greater photosynthetic CO_2 assimilation than *Ma* under the control, but there was no significant difference between *Ma* and *Bp* in the absorption rate of bicarbonate (Tables 1, 2). The changes in V_{SFW} and photosynthetic CO_2 assimilation capabilities of the two plant species under 24L and 24D were inconsistent. Non parallel in bicarbonate uptake and photosynthetic CO_2 assimilation of plants indicated that the conversion of karst carbon sinks into photosynthetic carbon sequestrations did not affect photosynthetic CO_2 assimilation per unit leaf area.

The absorption and utilization of bicarbonate by plants throughout the day may result from the PEPC and Rubisco contents (Figure 2). It has been reported that DIC carbon fixation in roots is related to PEPC (Vuorinen *et al.* 1989; Vuorinen *et al.* 1992). The role of PEPC in root bicarbonate

absorption and utilization is related to the conversion of malic acid. Malic acid is formed from PEPC and/or phosphoenolpyruvate carboxykinase (PEPCK) in the roots (Popp *et al.* 1982). Bicarbonate is absorbed and utilized by plants *via* the function of PEPC, which is considered a nonphotosynthetic pathway.

A previous study proved that Rubisco in leaves can combine CO_2 from the conversion of root-derived bicarbonate to form carbohydrates during photosynthesis under light (Wu and Xing 2012; Rao and Wu 2017). In this study, we found that there were considerable amounts of Rubisco in the leaves under 24D, even more than under 24L (Table 3), which seemed to question the role of Rubisco in bicarbonate absorption and utilization. However, it has been reported that the expression of the Rubisco chaperone gene in cyanobacterial blooms reached its highest expression during darkness and was downregulated during the daytime (Sandrini *et al.* 2016). Therefore, Rubisco reacts and is consumed only under light and does not function as carboxylation in the dark. Bicarbonate is absorbed and utlized by plants *via* the function of Rubisco, which is considered a photosynthetic pathway.

The synergism in the absorption and utilization of photosynthetic pathway and nonphotosynthetic pathway dominated the transformation of the karst carbon sinks of plants. *Ma* can absorb more bicarbonate than *Bp* (Table 1). However, bicarbonate is greatly alkaline, and too much absorption and too little utilization by plants will cause damage to plants. In addition to less absorption of bicarbonate than *Ma*, the absorbed bicarbonate of *Bp* can be more readily used as a carbon source for photosynthetic organs to further reduce the damage of bicarbonate to plants because the capability of *Bp* to convert bicarbonate into CO_2 and water by carbonic anhydrase (CA) is stronger than that of *Ma*. A previous study showed that approximately 30% of the photosynthetic products of *Bp* come from CO_2 transformed from bicarbonate by CA, while only 0%–15% of those of *Ma* arise this way (Wu and Xing 2012). The involvement of the photosynthetic pathway vs the nonphotosynthetic pathway in bicarbonate uptake was greater in *Bp* than in *Ma*, which prevented the accumulation of organic acids from diminishing the adverse effect of growth in *Bp*. The moderate absorption and massive utilization of bicarbonate by *Bp* greatly reduced the damage. *Ma* is difficult to grow in karst regions, which is related to its high nonphotosynthetic absorption and low photosynthetic utilization of bicarbonate. This result is consistent with previous findings that *Bp* is a karst-adaptable plant (Zhao and Wu 2018).

The two plant species absorbed and utilized more bicarbonate under 24L than 24D (Table 1), indicating that light can promote the absorption and utilization of bicarbonate by plants, which proves that uptake of bicarbonate occurs through the xylem with transpiration flow to the shoots. It has been previously reported that bicarbonate may be incorporated into xylem proteins and transported to the shoots (Mengel *et al.* 1994; Wegner and Zimmermann 2004), and HCO_3^- in xylem sap may be the carbon source of Rubisco in leaves (Popp *et al.* 1982; Stringer and Kimmerer 1993).

The greater bicarbonate uptake in *Bp* with a smaller R/S suggested that the absorption and utilization of bicarbonate is related to transpiration in leaves. *Bp* with a smaller R/S absorbed more bicarbonate, which will cause more free HCO_3^- and increase the toxic effect in the plants (Table 1). Therefore, *Bp* with a larger R/S has better karst adaptation than that with a smaller R/S.

One of 2 moles of bicarbonate taken up by plants originated from CO_2 in the air during karst corrosion (Figure 2). This part of the carbon flux should be included in the global carbon budget. This pathway may lead to a larger carbon flow during all times of day and play an important role in the global carbon cycle, a role which has previously been underestimated. On the one hand, plants use bicarbonate to drive the corrosion of the carbonate and accelerate the formation of a carbon sink of corrosion, which makes a huge contribution to carbon neutrality. On the other hand, this is conducive to plant growth, increases the carbon sequestration capacity of plants, and provides organic matter and energy for the ecosystem. Karst-adaptable plants are especially able to regulate the entire carbon cycle. Therefore, quantifying the transformation of karst carbon sinks into carbon sequestrations by plants can not only provide new knowledge for the carbon metabolism of plants but also provide basic data for screening karst-adaptable plants and may ultimately provide a new solution for carbon peaks and carbon neutrality. The coupled relationship between the plant inorganic and organic carbon cycles is the key to modifying the carbon circulation model, especially in karst regions.

5. Conclusion

The bidirectional isotope tracer technique can quantify the absorption and utilization of root-derived bicarbonate. The tremendous karst carbon sinks can be transformed into carbon sequestrations by plants *via* photosynthetic and nonphotosynthetic pathway. Karst-adaptable plants can increase carbon sequestrations through the transformation to strengthen both karst and vegetation carbon sinks in the karst ecosystem.

Disclosure statement

No potential conflict of interest was reported by the author(s).

Funding

This work was supported by the National Natural Science Foundation of China [number U1612441-2] and Support Plan Projects of Science and Technology of Guizhou Province [number (2021)YB453].

Notes on contributors

Lei Fang is a PhD student studying in the Institute of Geochemistry, Chinese Academy of Sciences.

Yanyou Wu is a Professor working in the Institute of Geochemistry, Chinese Academy of Sciences.

References

Bloom P, Inskeep W. 1986. Factors affecting bicarbonate chemistry and iron chlorosis in soils. J Plant Nutr. 9(3):215–228.

Boxma R. 1972. Bicarbonate as the most important soil factor in lime-induced chlorosis in Netherlands. Plant Soil. 37(2):233–243.

Cao M, Prince SD, Li K, Tao B, Small J, Shao X. 2003. Response of terrestrial carbon uptake to climate interannual variability in China. Glob Change Biol. 9(4):536–546.

Carvalhais N, Forkel M, Khomik M, Bellarby J, Jung M, Migliavacca M, Mu M, Saatchi S, Santoro M, Thurner M, et al. 2014. Global covariation of carbon turnover times with climate in terrestrial ecosystems. Nature. 514(7521):213–217.

Ciais P, Denning AS, Tans PP, Berry JA, Randall DA, Collatz GJ, Sellers PJ, White JWC, Trolier M, Meijer HAJ, et al. 1997. A three-dimensional synthesis study of $\delta^{18}O$ in atmospheric CO_2: 1. Surface fluxes. J Geophys Res Atmos. 102(D5):5857–5872.

Farquhar GD, Lloyd J, Taylor JA, Flanagan LB, Syvertsen JP, Hubick KT, Wong SC, Ehleringer JR. 1993. Vegetation effects on the isotope composition of oxygen in atmospheric CO_2. Nature. 363(6428):439–443.

Friedlingstein P, O'Sullivan M, Jones MW, Andrew RM, Hauck J, Olsen A, Peters GP, Peters W, Pongratz J, Sitch S, et al. 2020. Global Carbon Budget 2020. Earth Syst Sci Data. 12(4):3269–3340.

Jiang ZC, Yuan DX. 1999. CO_2 source-sink in karst processes in karst areas of China. Episodes. 22(1):33–35.

Law BE, Falge E, Gu L, Baldocchi DD, Bakwin P, Berbigier P, Davis K, Dolman AJ, Falk M, Fuentes JD, et al. 2002. Environmental controls over carbon dioxide and water vapor exchange of terrestrial vegetation. Agric For Meteorol. 113(1-4):97–120.

Liu J, Zhong J, Chen S, Xu S, Li SL. 2021. Hydrological and biogeochemical controls on temporal variations of dissolved carbon and solutes in a Karst River, South China. Environ Sci Europe. 33(1).

Lu F, Hu HF, Sun WJ, Zhu JJ, Liu GB, Zhou WM, Zhang QF, Shi PL, Liu XP, Wu X, et al. 2018. Effects of national ecological restoration projects on carbon sequestration in China from 2001 to 2010. Proc Natil Acad Sci U S A. 115(16):4039–4044.

Luo ZK, Luo YQ, Wang GC, Xia JY, Peng CH. 2020. Warming-induced global soil carbon loss attenuated by downward carbon movement. Glob Chang Biol. 26(12):7242–7254.

Maxwell K, Johnson GN. 2000. Chlorophyll fluorescence—a practical guide. J Exp Botany. 51(345):659–668.

Mengel K, Planker R, Hoffmann B. 1994. Relationship between leaf apoplast pH and iron chlorosis of sunflower (*Helianthus annuus L.*). J Plant Nutr. 17(6):1053–1065.

Millero FJ. 2014. Physico-chemical controls on seawater. In: Heinrich DH, Karl KT, editors. Treatise on geochemistry. 2nd ed. Miami, FL, USA: Elsevier; p. 1–18.

Philip VB, Townsend K. 2005. A disturbance index for karst environments. Environ Manage. 36(1):101–116.

Popp M, Osmond CB, Summons RE. 1982. Pathway of malic acid synthesis in response to ion uptake in wheat and lupin roots evidence from fixation of ^{13}C and ^{14}C. Plant Physiol. 69:1289–1292.

Ran L, Butman DE, Battin TJ, Yang X, Tian M, Duvert C, Hartmann J, Geeraert N, Liu S. 2021. Substantial decrease in CO_2 emissions from Chinese inland waters due to global change. Nat Commun. 12(1):1730.

Rao S, Wu YY. 2017. Root-derived bicarbonate assimilation in response to variable water deficit in Camptotheca acuminate seedlings. Photosynth Res. 134(1):59–70.

Raymond PA, Hartmann J, Lauerwald R, Sobek S, McDonald C, Hoover M, Butman D, Striegl R, Mayorga E, Humborg C, et al. 2013. Global carbon dioxide emissions from inland waters. Nature. 503(7476):355–359.

Sandrini G, Tann RP, Schuurmans JM, van Beusekom SA, Matthijs HC, Huisman J. 2016. Diel variation in gene expression of the CO_2-concentrating mechanism during a harmful cyanobacterial bloom. Front Microbiol. 7:551.

Stringer JW, Kimmerer TW. 1993. Refixation of xylem sap CO_2 in *Populus deltoide*. Physiol Plant. 89(2):243–251.

Tong X, Brandt M, Yue Y, Horion S, Wang K, Keersmaecker WD, Tian F, Schurgers G, Xiao X, Luo Y, et al. 2018. Increased vegetation growth and carbon stock in China karst *via* ecological engineering. Nat Sustainability. 1(1):44–50.

Vuorinen AH, Vapaavuori EM, Lapinjoki SP. 1989. Time-course of uptake of dissolved inorganic carbon through willow roots in light and in darkness. Physiol Plant. 77:33–38.

Vuorinen AH, Vapaavuori EM, Raatikainen O, Lapinjoki SP. 1992. Metabolism of inorganic carbon taken up by roots in *Salix* plants. J Exp Botany. 43(251):789–795.

Wang S, Grant RF, Verseghy DL, Black TA. 2001. Modelling plant carbon and nitrogen dynamics of a boreal aspen forest in CLASS — the Canadian land surface scheme. Ecol Modell. 142(1-2):135–154.

Wang SJ, Liu QM, Zhang DF. 2004. Karst rocky desertification in southwestern China: geomorphology, landuse, impact and rehabilitation. Land Degrad Dev. 15(2):115–121.

Wegner LH, Zimmermann U. 2004. Bicarbonate-induced alkalinization of the xylem sap in intact maize seedlings as measured in situ with a novel xylem pH probe. Plant Physiol. 136(3):3469–3477.

Weis E, Berry JA. 1987. Quantum efficiency of photosystem II in relation to 'energy'-dependent quenching of chlorophyll fluorescence. Biochim Biophys Acta. 894(2):198–208.

Wu YY, Xing DK. 2012. Effect of bicarbonate treatment on photosynthetic assimilation of inorganic carbon in two plant species of Moraceae. Photosynthetica. 50(4):587–594.

Yan JH, Li JM, Ye Q, Li K. 2012. Concentrations and exports of solutes from surface runoff in Houzhai Karst Basin, southwest China. Chem Geol. 304-305:1–9.

Yao K, Wu YY. 2021. Rhizospheric bicarbonate improves glucose metabolism and stress tolerance of *Broussonetia papyrifera L.* seedlings under simulated drought stress. Russian J Plant Physiol. 68(1):1021–4437.

Zhao K, Wu YY. 2017. Effects of Zn deficiency and bicarbonate on the growth and photosynthetic characteristics of four plant species. Plos One. 12(1). e0169812.

Zhao K, Wu YY. 2018. Effect of Zn deficiency and excessive bicarbonate on the allocation and exudation of organic acids in two Moraceae plants. Acta Geochimica. 37(1):125–133.

Zhu Z, Piao S, Myneni RB, Huang M, Zeng Z, Canadell JG, Ciais P, Sitch S, Friedlingstein P, Arneth A, et al. 2016. Greening of the Earth and its drivers. Nat Climate Change. 6(8):791–795.